

Characterization of fine fraction of Municipal Solid Waste Incineration Bottom Ash (MSW IBA) focused on pure aluminum and copper recovery

H. Muñiz¹, M. Šyc¹, J. Výravský²

¹Department of Environmental Engineering, Institute of Chemical Process Fundamental of the Czech Academy of Sciences, v. v. i., Prague, 165 02, Czech Republic

²TESCAN Brno, Brno, 623 00, Czech Republic

Presenting author email: muniz@icpf.cas.cz

ABSTRACT

Results of an extensive analysis of the abundance, shape and liberation grade of the aluminum and copper particles present in the incineration bottom ash (IBA) fine fraction, up to 2 millimeters, from a municipal solid waste incineration plant is presented. The total amount of aluminum and copper related to the IBA particle size fraction have been analyzed in order to propose different possibilities of separation technology for their recovery.

It is shown that the aluminum content, 1655 grams per ton, is considerably higher than copper content (610 grams per ton). The amounts of metals are unequally distributed in the residue: more than 75% wt. of copper and 55%wt. of aluminum are in the fine fraction between 0.1 to 1.0 millimeters. Compared with aluminum, the shape of copper grains has a bigger ellipse ratio (the maximum height/width ratio of a grain) and they are the least liberated. In addition, no copper grains bigger than 1 millimeter were detected.

This big amount of non-ferrous metals makes its recovery a profitable industry. According to the parameters analyzed and the physicochemical properties of these non-ferrous metals, electrostatic technologies are suitable to produce a high purity non-ferrous metals fraction, in addition, gravimetric concentration systems could be used for copper pre-concentration or separation and recovery of high purity non-ferrous metals fractions.

KEYWORDS:

Incineration Bottom Ash, metal recovery, recycling, circular economy.

1. INTRODUCTION

In the year 2012, the amount of Municipal Solid Waste (MSW) generated was 1.3 billion tons. With 2.9 billion of urban population and an expected gradual increase of population, more than 2.2 billion tons of waste is expected to be generated in 2025 [1]. Different technologies and processes are being used for its management including incineration, landfilling, recycling and composting. The continuous technology development, the lack of storage capacity in landfills, and environmental awareness have made the Municipal Solid Waste Incineration (MSWI) Technology an interesting solution [2]. Compared with the direct landfilling of MSW, the landfilled mass after MSWI is 70% lower (volume by 90%) [3].

In the EU-28, the use of Municipal Solid Waste Incineration Plants (MSWI-Plants) has increased during the last 20 years: in 2016 approximately 68 million tons was incinerated, implying an increment of 112% during these years [4]. The rate and type of material in the MSW closely depends on the countries income. Higher income countries are the biggest producers, however, these regions achieve lower amount of organic compounds. Table 1 presents on detail these variations.

Table 1 Rate and type of waste material related to the country income [1].

	High Income (%)	Upper Middle Income (%)	Lower Middle Income (%)	Lower Income (%)
Global Waste Generation	46	19	29	6
Organic Fraction	59	68	68	69
Plastic Fraction	11	11	12	8
Glass Fraction	7	5	3	3
Metal Fraction	6	3	2	3
Other Fractions	17	13	15	17

Incineration is usually not the last step of the treatment. This process mainly generates two types of residues: Incineration Bottom Ash (IBA) and Incineration Fly Ash (IFA). In summary, the IFA is formed by the finer or lighter particles generated in the combustion chamber which are entrained by the stream of flue gases and the IBA composed of larger and heavier particles that remain on the furnace grate. Approximately 70% of the Municipal Solid Waste mass is combustible material, 25% is IBA and the rest is IFA [5]. The management of these materials mainly includes the heavy metals immobilization, material recovery and the use of these residues in other industries. Even with the reduction of residues dumped in landfills, the management of these residues is considered a critical environmental factor. Several compounds in the IFA, like heavy metals (lead, zinc or antimony), chloride salts or other compounds are potential contaminants, and they are usually captured by different technologies like electrostatic precipitators, cyclones, and bag filtered [6, 7].

IBA is a non-hazardous residue composed by a mix of glass, minerals, and metals which mainly depend on the type of MSW incinerated, the type of quenching and the cooling time and the storage conditions. Among the different potential problems, ions leachability control and more specifically the heavy metals leachability is one of the most important factors to be controlled. This factor has been studied in different aspects such as heavy metals leachability in the landfills, its control in applications as a suitable material on the pavements or construction materials [8, 9, 10], or the capacity of some of the IBA compounds for the immobilization of heavy metals [11].

Recycling and reuse of these residues are incorporated in the circular economy, defines as a regenerative system in which resource input and waste, emission, and energy leakage are minimized by slowing, closing, and narrowing material and energy loops. This can be achieved through long-lasting design, maintenance, repair, reuse, remanufacturing, refurbishing, and recycling. [12]. Based on this philosophy, the recovery and reuse of some of the existing materials in IBA are an interesting strategy. Technologies and processes have been used for the residue utilization, and material recovery: Several applications as fill or sub-base in different uses like pavements industry [13, 14, 15], as a suitable aggregate for concrete [16, 17, 18] or ceramic industry [19] and, in some cases, for the recovery of different metals [20]. Other more specific uses and processes have been studied as its application as an activator for methane production [21] or its use as a sorbent material for heavy metal ions adsorption [22]. Previous of these applications, in some cases, IBA treatment plants incorporate different Advanced Recycling System mainly centered on the recovery of ferrous and non-ferrous metals, in addition, rare earth and precious metals are being recovered.

Economically, the recovery of ferrous and non-ferrous metals of the IBA is a profitable industry. The prices of the different metals like aluminum 1839\$/ton, copper 5860\$/ton, zinc 2467\$/ton, nickel 11415\$/ton or gold 1291.1\$/oz. which ones have shown a constant increase in the last three years [23]. The recovery capacity of each material is a critical factor for the economic viability of the recycling process, this recovery potential is mainly based on the amount of product in the residue, its particle size, the liberation grade of the material, the technical capacity of the recovery devices, and separation cost. Generally, the lower the particle size and liberation grade, the more difficult is the separation.

Residue composition researches are focused on its mineralogical composition and metal presence related to the residue particle size. These characteristics are relevant for the design of the different recovery treatments. Different studies have analyzed some of these factors: Šyc et al. and Loginova et al. [24, 25] analyzed in detail the IBA composition in

different granulometric fraction focused on the abundance of metals, Muchova et al. [26] have studied the presence of precious metals in the IBA and the technical and economic viability of its recovery. Presence of rare earth metals on the MSW has been studied [27]. Nevertheless, the abundance of metals in the finest fraction with the focus on the possibility of their recovery has so far not been well studied. Del Valle-Zermeño et al. [28] divided the IBA finest fraction into two particle sizes (1-2mm and <1mm). Similarly, Xia et al [29] studied the metal composition of the bottom ash and, in their study, divided the finest fraction into two parts (1-3mm and <1mm). These researchers found by the analysis of several IBA fine fraction, up to 3 millimeters, a high amount of the metals (20-40% wt. of aluminum, 40% wt. of ferrous metals, 45-80% wt. of copper or 45-75% wt. of Zinc). These high content made the non-ferrous metals recovery in the IBA fine fraction a profitable industry.

The IBA metals are in some cases in the form of metal alloys, minerals or other amorphous compounds. Most of these metals are embedded into large particles (usually inner a glass matrix) or sticking in the particle boundary [30, 31]. From an economical, technical and industrial point of view, metal recovery is directly related to the particle size, its shape, the liberation grade of the material and its abundance. In most of the cases the industries have achieved the recovery of the ferrous and non-ferrous metals presented in the coarse fraction of the residue, however, the finest fraction is not treated. The present investigation has obtained the amount of pure copper and aluminum present in the finest fraction of the IBA, up to 2 millimeters. Based on the characteristics analyzed (amount of metal, size and shape of the grains and degree of release), various equipment and treatments have been proposed for the recovery of aluminum and copper.

2. MATERIAL AND METHODS

IBA metal recovery possibilities largely depend on the particle size. For that reason, a granulometric distribution size analysis of the IBA fine fraction, up to 2 millimeters, has been realized in order to obtain the amount of metal present in each fraction. A total of 54 samples collected from several Waste-to-Energy plants from the Czech Republic.

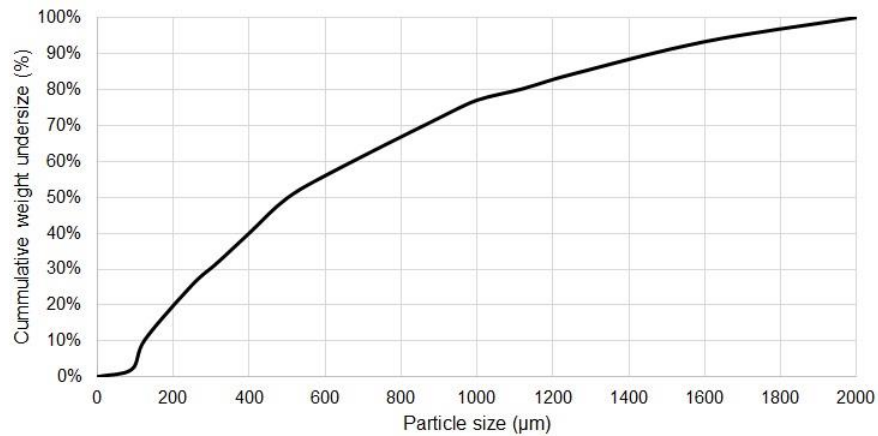
Mineral analysis of the residue has been realized by TESCAN Brno, s.r.o with its technology denominated TIMA (TESCAN Integrated Mineral Analyzer). The device combines signals from the BSE detector and up to 4 EDS detectors to distinguish chemically distinct phases and to create images of mineral grains and particles, which are quantitatively evaluated in dedicated software [32]. Besides that, the device is equipped with additional analytical tools like WDS (wavelength dispersion spectroscopy), CL (cathodoluminescence), EBSD (electron backscatter diffraction) or Raman spectrometer to provide more comprehensive and correlative analysis of the sample. Due to the IBA composition heterogeneity, the amount of copper and aluminum on the IBA fine fraction, below 2 millimeters, has been obtained based on different samples collected on the in Waste-to-Energy plants of the Czech Republic. Granulometric distribution size analysis was made with a sample of this residue.

2.1. Particle size distribution analysis:

Several samples were analyzed coming from different MSWI-Plants in the Czech Republic in order to obtain the average weight percentage of material below 2 millimeters which average is 35% of the total amount of the IBA [24]. This fact confirms the high interest in the treatment of this fraction. Particle size distribution analysis of this fine fraction is presented (Figure 1), where its d_{50} parameter (the size in microns that divide equally the accumulated weight) is 505 microns. Besides that, d_{25} and d_{75} (size in microns which 25% and 75% of the cumulative weight have lower size) are 245 and 957 microns.

According to an optimum particle size for different possible separation devices, four granulometric fractions have been studied: Below 100 microns which represents less than 5% wt. of the IBA fine fraction, between 100 to 500 microns which is approximately 45% wt., between 0.5 to 1.0 millimeters (near 30% wt.) and a coarse fraction with particles bigger than 1.0 millimeters which represents less than 25% wt. of IBA.

Fig.1 Grain size distribution of the fine fraction of IBA below 2 millimeters



2.2. Analysis method:

The separated particles were mounted into 30 mm diameter, rounded, epoxy resin blocks and polished. The blocks were coated with 25 nm layer of carbon prior to analysis to prevent charging. Twenty blocks from the finer fraction (<0.5 mm) and 34 blocks from the coarser fraction (0.5-2 mm) were analyzed by TIMA. The following analytical conditions were used: Acceleration voltage 25 kV, probe current 10 nA, working distance 15 mm, EDAX Element SDD EDS detectors calibrated to 600 000 cts/s input count rate (on Platinum). The samples were analyzed by liberation analysis- high-resolution mapping mode (same grid for BSE and EDS pixels [32]) with a pixel spacing of 4 µm. The densities of phases from publicly available mineral and material databases and theoretical compositions (for native metals and simple compounds) or mean composition of several tens of biggest grains obtained by standard-less semiquantitative EDS analysis built in TIMA (for glasses and other complicated phases) were assigned to the phases in the TIMA software to calculate mass content and department of the metals of interest. The grain or particle size in TIMA are expressed as ECD (Equivalent Circle Diameter), which is the diameter of a circle, which would have the same area as the measured grain or particle. The data were analyzed and outputs were generated in TIMA 1.6.36 software version.

3. RESULTS:

3.1. Analysis of the pure copper mass in the IBA fine fraction.

Copper abundance analysis of the IBA fine fraction showed that the total amount of copper was approximately 0.6 grams per kilogram. Metal abundance is unequally distributed in this fraction: Copper grains (defined as a single mass only composed by this metal) had mostly sizes between 0.1 to 1.0 millimeters, no grains bigger than 1.0 were detected. Approximately the same amount of copper was detected in particle size fractions (particle defined as the agglomerate of different grains forming a single mass) between 0.1 to 0.5 millimeters and 0.5 to 1.0 millimeters which were more than 75% wt. of the IBA fine fraction. No metal grains were found in the fraction bigger than 1.0 millimeters, however, almost 20% wt. of copper was in this particle size fraction. Copper fraction, defined as the amount of pure metal related to the IBA fraction weight, was similar in all fractions, approximately 0.05% wt. This factor only increased up to 0.08% wt. in the particle fraction between 0.5 to 1.0 millimeters. Metal distribution and fraction are detailed in Table 2 and Figure 2. Mineralogical analysis of these fraction indicated that 85% of copper was pure with a high abundance of oxides and chloride phases. Mineralogical phases are detailed in Table 3.

Fig.2 Pure copper mass distribution according to the grain and particle.

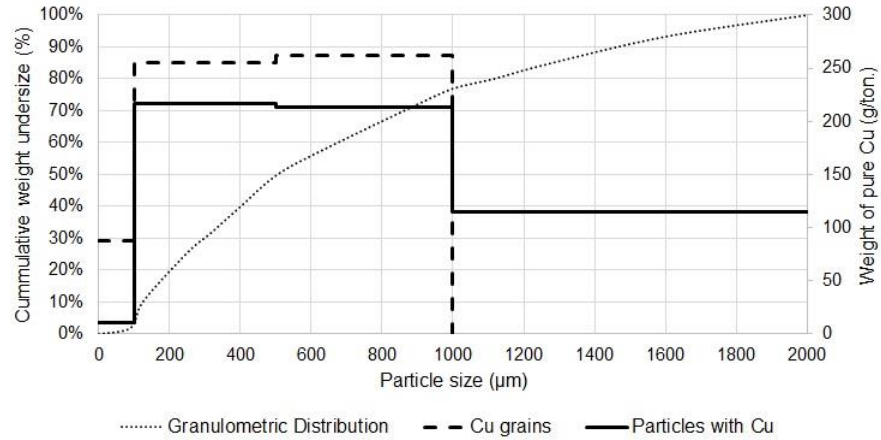


Table 2 Mass and copper fraction related to the particle size fraction of the IBA.

Particle size (µm)	Mass fraction (%)	Copper mass (mg/kg)	Copper fraction (%)
< 100	5	28	0,06
100-500	45	217	0,05
500-1000	27	213	0,08
1000-2000	23	114	0.05

Copper grain shape analysis showed a high amount of singular grains (more than 40% wt.) with ellipse ratio between 2/10 to 3/10. This shape relation could be due to a high presence of small pieces of wire copper, which ones could explain the no existence of copper larger than 1.0 millimeters, which ECD is below 1 millimeter. However, according to the analysis, these grain shapes were more abundant in the smaller metal grains, up to 0.5 millimeters. Approximately 20% wt. of the copper grains had an ellipse ratio between 6/10 to 7/10. An example of several copper grain shapes analyzed is represented in Figure 3. Copper liberation rate in the residue (defined as the volume of metal grain related with the total volume of the particle) showed that more than 60% wt. of the grains had a liberation rate higher than 60% vol. This factor is closely dependent on the metal particle size: more than 75% wt. of pure copper particles up to 0.5 millimeters had a liberation rate higher than 70% vol., this rate was different in the coarse fraction, where more than 55% wt. of pure copper particles had a liberation rate between 30% to 40% vol. and just 22% wt. have a liberation rate between 70 to 80%. No coarse copper particles had a liberation rate higher than 80%. Figure 4 represents in detail the liberation rate and ellipse ratio of copper-containing particles.

Fig.3 Samples of the copper grain shapes in the IBA

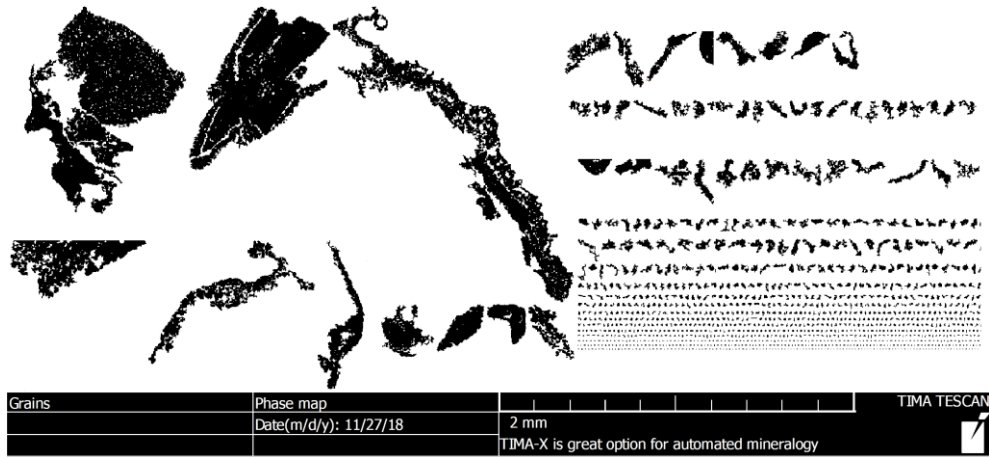
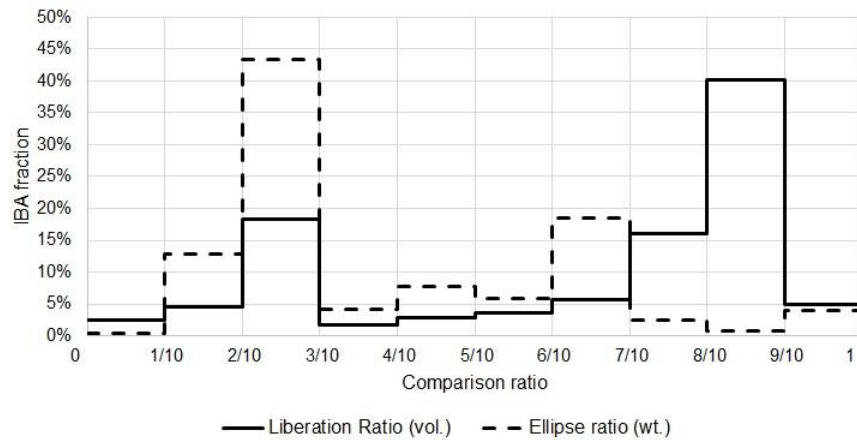


Fig.4 Copper Liberation and Ellipse ratio



3.2. Analysis of the pure aluminum mass in the IBA fraction below 2mm

Residue analysis revealed that the pure aluminum metal in the IBA fine fraction was nearly 1.60 grams per kilogram. According to the different mineralogical components that are formed, pure aluminum and its alloys represent approximately 20% wt. in metal grains between 0.5 to 2.0 millimeters, which decreases up to the 10% wt. in the fine grains. Otherwise, glass and silicate phases and an important presence of aluminum oxide were the most abundant fraction of aluminum components. Mineralogical characterization of the aluminum abundance is shown in detail on Table 3.

Table 3 Copper and Aluminum mineralogical phases.

Grain size (mm)	Copper phases (%)		Aluminum phases (%)	
	< 0,5mm	0,5-2,0mm	< 0,5mm	0,5-2,0mm
Native metals and alloys	88,12	84,37	9,49	18,14
Oxides, chlorides and other phases	7,30	11,12	34,55	22,48
Glass and silicate phases	4,14	3,82	55,32	59,02
Phosphates, sulphates and carbonates	0,44	0,69	0,64	0,36

More than 50% wt. of the pure aluminum grain size was between 100 and 500 microns, in addition, only 5% wt. of these grains were below 100 microns. There were no important differences in the mass of the pure aluminum grains in the coarse fraction with particles bigger than 0.5 millimeters. A bigger amount of aluminum, approximately 40% wt., was detected in the particles containing aluminum bigger than 1.0 millimeters. 35% wt. of this metal was detected in the IBA fine fraction between 100 to 500 microns and just the 5% wt. was in the finest fraction. Figure 5 shows the relation between the size of the particles and aluminum grains with the amount of pure metal in each particle size fraction. Aluminum fraction (the amount of pure metal related to the IBA weight) was similar for the three particle size fractions up to 1.0 millimeters (between 0.12 to 0.15% wt.), while in the coarse particle fraction, this factor was relatively higher. Table 4 shows in detail the aluminum fraction and mass according to the different particle size fractions.

Fig.5 Pure aluminum mass distribution in function of the grain and particle size.

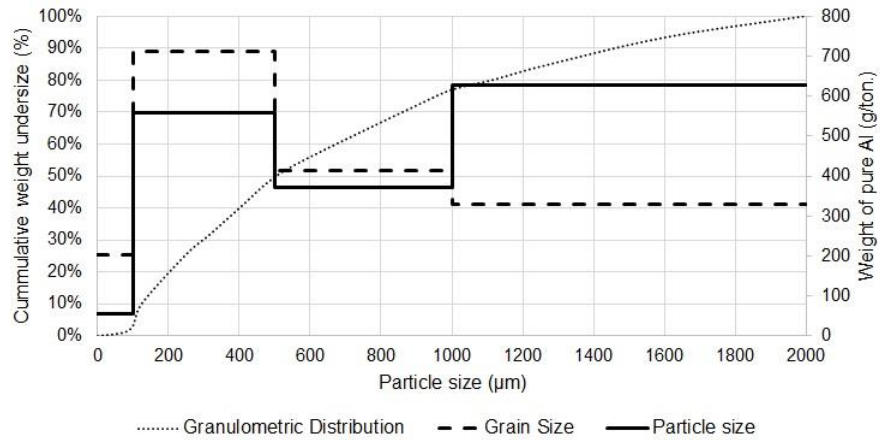


Table 4 Mass and purity fraction related to the particle size fraction of the IBA.

Particle size (µm)	Mass fraction (%)	Aluminum mass (mg/kg)	Aluminum fraction (%)
< 100	5	73	0,15
100-500	45	559	0,12
500-1000	27	370	0,14
1000-2000	23	629	0,27

Aluminum grain shape analysis conclude that, compared with the copper grains, aluminum particles had in most of the cases an ellipse ratio closer to one. More than 60% wt. of pure aluminum grains had an ellipse ratio bigger than 5/10 and no particles were detected between under 2/10 ellipse ratios. Examples of shape and size of several pure aluminum grains analyzed are represented in Figure 6. Less than 35% wt. of the particles had a liberation grade below than 50% vol. Besides that, 37.4% wt. of the particles had a liberation rate higher than 70% vol. These values depend closely on the particle size: liberation rate in the fine particles (below 0.5 millimeters) was lower, less than 30% of aluminum particles had a liberation rate lower than 70%, however, liberation was higher than 50% in the coarse fraction between 0.5 to 2.0 millimeters. Figure 7 represents more detail the ellipse and liberation ratio related to the pure metal proportion.

Fig.6 Samples of the copper grains shape in the IBA residue

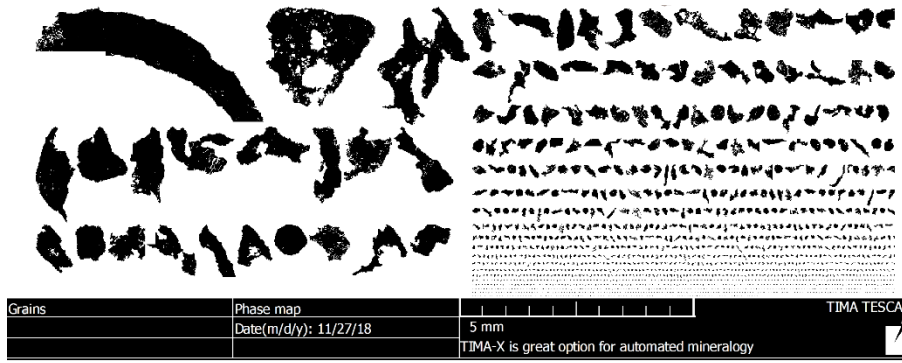
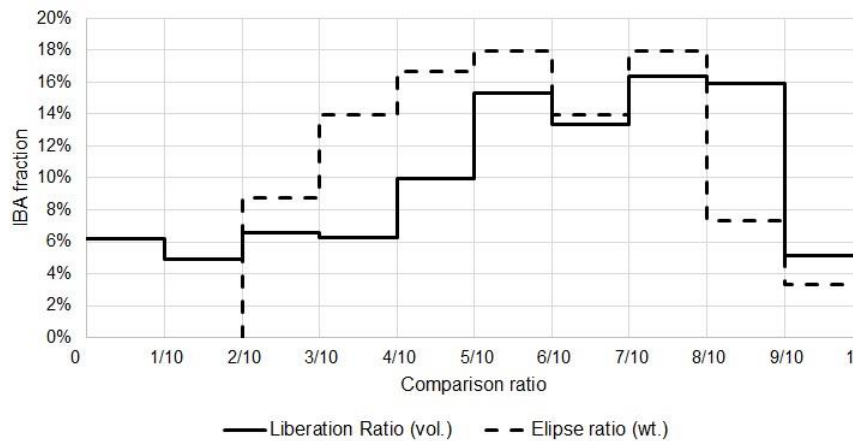


Fig.7 Aluminum Liberation and Ellipse ratio



4. DISCUSSIONS:

The amount of pure aluminum and copper and its proportion related to the other mineralogical phases showed in this study support the results obtained by different researchers [33, 34]. The mass of pure metal grains increased with the particles size. In both cases, the smallest amount of metals was detected in the fine fraction up to 100 microns, however, this fraction did not have the lower metal fraction. Approximately 60% wt. of pure aluminum and copper were in the particles bigger than 500 microns.

Copper abundance in the IBA fine fraction, 610 grams per ton, and the aluminum phases are similar to those found by other researchers. Pure copper and its alloys formed the most abundant phase in the copper residue, besides that, its abundant did not differ with the size of the grains. Above 1655 grams per ton of pure aluminum was detected in this IBA fine fraction. Oxides and chloride phases are the most abundant aluminum compounds, significantly higher than the pure or alloys representing less than 20% wt. The aluminum phases were significantly related to the grain size. Aluminum reactivity could explain these facts forming different compounds, like aluminosilicates or aluminum sulfates (microcline or ettringite) and a great abundance of its oxide form, alumina (Al_2O_3) [35,36]. Metal abundance related to the particle size fraction and the metal fraction parameter is detailed in Table 5.

Copper shape analysis indicated that more than 55% wt. have an ellipse ratio higher than 3/10. This result explains the no detection of copper grains bigger than 1 millimeter: large particles with this high ellipse ratio have an ECD is lower than one millimeter. Aluminum shape grain analysis concluded that, compared with the copper grains, aluminum particles had in most of the cases an ellipse ratio closer to one. This relation was bigger than 5/10 for more than 60% wt. of the aluminum grains, besides that, no metal grains were detected with an ellipse ratio lower than 2/10.

The liberation rate is unequally distributed: more than 60% wt. of copper particles had a liberation rate higher than 80% vol., however, this amount was lower than 40% wt. for the aluminum particles. Fine copper particles, up to 500 microns, were more liberated than the coarse ones, while this factor was not significant for the aluminum particles.

According with the particle characteristics, the efficiency on concentration devices mainly depends on the shape and particle size of the product to recover, the amount of material to extract, and its liberation grade: the first two factors are critical for the selection of the concentration device while the last is an important factor in the recovery and purity of the product obtained. The grinding process could be applicable to improve the liberation grade and the treatment efficiency, however, this process has a high energy consumption which could worsen the profitability of the separation process [37]. Other properties and characteristics as conductivity or material density are critical factors for the treatment design. Gravimetric concentration systems are highly effective treatments that take advantage of the material density in order to produce a high purity fraction with a low operation cost. Copper density is greater than the average of the IBA particles. This difference could be harnessed by gravimetric concentration systems like shaker tables or jigs technologies that could produce a fraction formed by the densest compounds like heavy metals (copper, zinc, chrome...), magnetic components or precious metals. Aluminum density is close to the average of the IBA materials, this fact concludes that gravimetric technology could not be appropriate for this metal. Electrical and electrostatic separator devices exploit the electrical conductivity of the non-ferrous metals in order to produce a high purity fraction of metals. Particle size is a critical factor for this technologies: electrical separators are high efficiency with particles below 75 microns (high tension devices could operate particles up to 0.5 millimeters), however, these devices have a low capacity of treatment [38]. Eddy Current Separators could be used for the coarse fraction of the residue (bigger than 0.5 millimeters), this technology is widely used for the recovery of non-ferrous metals of particles between 0.5 to 2.5 millimeters. Hydrometallurgical treatments are extensively used for high purity copper recovery in the Waste Electrical and Electronic Residues (WEEE) or muds from copper mines [39, 40]. These technologies could be applicable too in the IBA fine fraction.

Table 5 Mass and metal fraction related to the particle size fraction of the IBA.

Pure metal or alloys (%)	Copper		Aluminum	
	< 0,5mm	0,5-2,0mm	< 0,5mm	0,5-2,0mm
	88,1	84,4	9,5	18,1
IBA granulometric fraction	Fraction of total pure metal (%)	Copper fraction (%)	Fraction of total pure metal (%)	Aluminum fraction (%)
< 100µm	4,9	0,06	4,5	0,15
100-500µm	38,0	0,05	34,3	0,12
500-1000µm	37,1	0,08	22,7	0,14
1000-2000µm	20,0	0,05	38,5	0,27

5. CONCLUSIONS:

Aluminum and copper amount in the IBA fine fraction below 2.0 millimeters has been studied. This quantity was 610 grams per ton for copper and 1650 grams per ton for aluminum. These amounts are similar to those found by other researchers. According to the IBA particle size, these non-ferrous metals were not evenly distributed in the waste: Lower fraction of pure metals, up to 6% wt., were in the fraction up to 0.1 millimeters, while the fraction between 0.1 to 0.5 millimeters, which was the highest amount of IBA fraction, represent approximately 37.9% wt. of copper and 34% of aluminum. Higher amounts of aluminum were found in the IBA below 1.0 millimeters.

The higher ellipse ratio of the coarse copper grains in the residue explain the no presence of copper particles bigger than 1.0 millimeters, besides that, aluminum particles had a more regular shape. Copper liberation rate was much higher than aluminum liberation rate, however, small copper grains were better liberated than the coarse grains. According to the possible compounds that could be formed with these two metals, pure copper and its alloys were the

most abundant, whereas silicates and oxides had a significantly more abundance in the aluminum. Pure aluminum represented less than 25% wt. of the total amount of compounds, maybe due to the high reactivity of this element.

Gravimetric concentration technologies could be appropriate for copper pre-concentration, nevertheless, this technology may not be applicable for the aluminum. Electrical separators are applicable for the finest fraction the IBA which only represent less than 5% wt. of the total IBA fine fraction, furthermore, some of these devices could be applicable for particles up to 500 microns. Eddy Current Separator could be suitable to obtain a high purity non-ferrous metals fraction. This technology could be applicable to particles between 0.5 to 2.5 millimeters. In addition, gravimetric technologies could be used for the separation of this non-ferrous metals fractions.

6. ACKNOWLEDGMENTS:

This work was supported by the Ministry of Education, Youth and Sports of the Czech Republic and EU - European Structural and Investment Funds - Operational Programme Research, Development and Education - project SPETEP (CZ.02.1.01/0.0/0.0/16_026/0008413) and INTER-COST project Mining the European Anthroposphere (LTC17051).

7. REFERENCES

- [1] Schuler, N., Casalis, A., Debomy, S., Johnnides, C., Kuper, K., Cointreau, S., ... Baeumler, A.: WHAT A WASTE - A Global Review of Solid Waste Manag. Washington DC (2012)
- [2] Abramov, S., He, J., Wimmer, D., Lemloh, M.-L., Muehe, E. M., Gann, B., ... Kappler, A.: Heavy metal mobility and valuable contents of processed municipal solid waste incineration residues from Southwestern Germany. Waste Manag. (2018) <https://doi.org/10.1016/J.WASMAN.2018.08.010>
- [3] Silva, R. V., de Brito, J., Lynn, C. J., & Dhir, R. K.: Use of municipal solid waste incineration bottom ashes in alkali-activated materials, ceramics and granular applications: A review. Waste Manag. (2017) <https://doi.org/10.1016/J.WASMAN.2017.06.043>
- [4] Eurostat. Municipal waste statistics. Statistics Explained. https://ec.europa.eu/eurostat/statistics-explained/index.php/Municipal_waste_statistics#Municipal_waste_treatment (2019). Accessed 18 January 2019
- [5] Brunner, P. H., & Rechberger, H.: Waste to energy – key element for sustainable waste management. Waste Manag. (2015) <https://doi.org/10.1016/J.WASMAN.2014.02.003>
- [6] Ko, M.-S., Chen, Y.-L., & Wei, P.-S.: Recycling of municipal solid waste incinerator fly ash by using hydrocyclone separation. Waste Manag. (2013) <https://doi.org/10.1016/J.WASMAN.2012.10.009>
- [7] Huang, T., Liu, L., Zhou, L., & Yang, K.: Operating optimization for the heavy metal removal from the municipal solid waste incineration fly ashes in the three-dimensional electrokinetics. Chemosphere (2018) <https://doi.org/10.1016/J.CHEMOSPHERE.2018.04.065>
- [8] Silva, R. V., de Brito, J., Lynn, C. J., & Dhir, R. K.: Environmental impacts of the use of bottom ashes from municipal solid waste incineration: A review. Resour., Conserv. and Recycl. (2019) <https://doi.org/10.1016/J.RESCONREC.2018.09.011>
- [9] Birgisdóttir, H., Pihl, K. A., Bhandar, G., Hauschild, M. Z., & Christensen, T. H.: Environmental assessment of roads constructed with and without bottom ash from municipal solid waste incineration. Transp. Res. (2006) <https://doi.org/10.1016/J.TRD.2006.07>
- [10] Cai, Z., Bager, D. H., & Christensen, T. H.: Leaching from solid waste incineration ashes used in cement-treated base layers for pavements. Waste Manag. (2004) <https://doi.org/10.1016/J.WASMAN.2004.01.010>

- [11] Wu, H., Wang, Q., Ko, J. H., & Xu, Q.: Characteristics of geotextile clogging in MSW landfills co-disposed with MSWI bottom ash. *Waste Manag.* (2018) <https://doi.org/10.1016/J.WASMAN.2018.05.032>
- [12] Geissdoerfer, M., Savaget, P., Bocken, N. M. P., & Hultink, E. J.: The Circular Economy – A new sustainability paradigm? *J. of Clean. Production.* (2017) <https://doi.org/10.1016/J.JCLEPRO.2016.12.048>
- [13] Le, N. H., Razakamanantsoa, A., Nguyen, M.-L., Phan, V. T., Dao, P.-L., & Nguyen, D. H.: Evaluation of physicochemical and hydromechanical properties of MSWI bottom ash for road construction. *Waste Manag.* (2018) <https://doi.org/10.1016/J.WASMAN.2018.09.007>
- [14] Lynn, C. J., Ghataora, G. S., & Dhir OBE, R. K.: Municipal incinerated bottom ash (MIBA) characteristics and potential for use in road pavements. *International J. of Pavement Res. and Technol.* (2017) <https://doi.org/10.1016/J.IJPRT.2016.12.00>
- [15] Luo, H.-L., Chen, S.-H., Lin, D.-F., & Cai, X.-R.: Use of incinerator bottom ash in open-graded asphalt concrete. *Constr. and Build. Mater.* (2017) <https://doi.org/10.1016/J.CONBUILDMAT.2017.05.164>
- [16] Lynn, C. J., Dhir OBE, R. K., & Ghataora, G. S.: Municipal incinerated bottom ash characteristics and potential for use as aggregate in concrete. *Constr. and Build. Mater.* (2016) <https://doi.org/10.1016/J.CONBUILDMAT.2016.09.132>
- [17] Kuo, W.-T., Liu, C.-C., & Su, D.-S.: Use of washed municipal solid waste incinerator bottom ash in pervious concrete. *Cem. and Concr. Composites.* (2013) <https://doi.org/10.1016/J.CEMCONCOMP.2013.01.001>
- [18] Li, X., Liu, Z., Lv, Y., Cai, L., Jiang, D., Jiang, W., & Jian, S.: Utilization of municipal solid waste incineration bottom ash in autoclaved aerated concrete. *Constr. and Build. Mater.* (2018) <https://doi.org/10.1016/J.CONBUILDMAT.2018.05.147>
- [19] Rambaldi, E., Esposito, L., Andreola, F., Barbieri, L., Lancellotti, I., & Vassura, I.: The recycling of MSWI bottom ash in silicate based ceramic. *Ceram. Int.* (2010) <https://doi.org/10.1016/J.CERAMINT.2010.08.005>
- [20] Xia, Y., He, P., Shao, L., & Zhang, H.: Metal distribution characteristic of MSWI bottom ash in view of metal recovery. *J. of Environ. Sci.* (2017) <https://doi.org/10.1016/J.JES.2016.04.016>
- [21] Yin, C., Shen, Y., Zhu, N., Huang, Q., Lou, Z., & Yuan, H.: Anaerobic digestion of waste activated sludge with incineration bottom ash: Enhanced methane production and CO₂ sequestration. *Appl. Energy.* (2018) <https://doi.org/10.1016/J.APENERGY.2018.02.056>
- [22] Wang, Y., Huang, L., & Lau, R.: Conversion of municipal solid waste incineration bottom ash to sorbent material: Effect of ash particle size. *J. of the Taiwan Inst. of Chem. Eng.* (2016) <https://doi.org/10.1016/J.JTICE.2016.09.026>
- [23] HKEX (n.d.). London Metal Exchange: Home. <https://www.lme.com/>. Accessed 18 January 2019.
- [24] Šyc, M., Krausová, A., Kameníková, P., Šomplák, R., Pavlas, M., Zach, B., ... Punčochář, M.: Material analysis of Bottom ash from waste-to-energy plants. *Waste Manag.* (2018) <https://doi.org/10.1016/J.WASMAN.2017.10.045>
- [25] Loginova, E., Volkov, D. S., van de Wouw, P. M. F., Florea, M. V. A., & Brouwers, H. J. H.: Detailed characterization of particle size fractions of municipal solid waste incineration bottom ash. *J. of Clean. Production.* (2019) <https://doi.org/10.1016/J.JCLEPRO.2018.10.022>
- [26] Muchova, L., Bakker, E., & Rem, P.: Precious Metals in Municipal Solid Waste Incineration Bottom Ash. *Water, Air, & Soil Pollut.: Focus.* (2009) <https://doi.org/10.1007/s11267-008-9191-9>
- [27] Morf, L. S., Gloor, R., Haag, O., Haupt, M., Skutan, S., Lorenzo, F. Di, & Böni, D.: Precious metals and rare earth elements in municipal solid waste – Sources and fate in a Swiss incineration plant. *Waste Manag.* (2013) <https://doi.org/10.1016/J.WASMAN.2012.09.010>

- [28] del Valle-Zermeño, R., Gómez-Manrique, J., Giro-Paloma, J., Formosa, J., & Chimenos, J. M.: Material characterization of the MSWI bottom ash as a function of particle size. Effects of glass recycling over time. *Sci. of the Total Environ.* (2017) <https://doi.org/10.1016/J.SCITOTENV.2017.01.047>
- [29] Xia, Y., He, P., Shao, L., & Zhang, H.: Metal distribution characteristic of MSWI bottom ash in view of metal recovery. *J. of Environ. Sci.* (2017) <https://doi.org/10.1016/J.JES.2016.04.016>
- [30] Kowalski, P. R., Kasina, M., & Michalik, M.: Metallic Elements Occurrences in The Municipal Waste Incineration Bottom Ash. *Energy Procedia.* (2017) <https://doi.org/10.1016/J.EGYPRO.2017.08.060>
- [31] Kowalski, P. R., Kasina, M., & Michalik, M.: Metallic Elements Fractionation in Municipal Solid Waste Incineration Residues. *Energy Procedia.* (2016) <https://doi.org/10.1016/J.EGYPRO.2016.10.013>
- [32] Hrstka, T., Gottlieb, P., Skála, R., Breiter, K., & Motl, D.: Automated mineralogy and petrology – applications of TESCAN integrated mineral analyzer (TIMA). *J. of Geosciences.* (2018) <https://doi.org/10.3190/jgeosci.250>
- [33] Seniunaite, J., & Vasarevicius, S.: Leaching of Copper, Lead and Zinc from Municipal Solid Waste Incineration Bottom Ash. *Energy Procedia.* (2017). <https://doi.org/10.1016/J.EGYPRO.2017.04.036>
- [34] Saffarzadeh, A., Arumugam, N., & Shimaoka, T.: Aluminum and aluminum alloys in municipal solid waste incineration (MSWI) bottom ash: A potential source for the production of hydrogen gas. *Int. J. of Hydrog. Energy.* (2016) <https://doi.org/10.1016/J.IJHYDENE.2015.11.059>
- [35] Kowalski, P. R., Kasina, M., & Michalik, M.: Metallic Elements Fractionation in Municipal Solid Waste Incineration Residues. *Energy Procedia.* (2016) <https://doi.org/10.1016/J.EGYPRO.2016.10.013>
- [36] Loginova, E., Volkov, D. S., van de Wouw, P. M. F., Florea, M. V. A., & Brouwers, H. J. H.: Detailed characterization of particle size fractions of municipal solid waste incineration bottom ash. *J. of Clean. Production.* (2019) <https://doi.org/10.1016/J.JCLEPRO.2018.10.022>
- [37] Menéndez, M., Muñoz Sierra, H., Gent, M., & de Cos Juez, F. J.: The comminution energy-size reduction of the Bond Mill and its relation to Vickers Hardness. *Miner. Eng.* (2018) <https://doi.org/10.1016/J.MINENG.2018.01.017>
- [38] Wills, B. A., Barry A., & Finch, J. A.: *Wills' mineral processing technology: an introduction to the practical aspects of ore treatment and mineral recovery*, Butterworth (UK) (2016)
- [39] Silvas, F. P. C., Jiménez Correa, M. M., Caldas, M. P. K., de Moraes, V. T., Espinosa, D. C. R., & Tenório, J. A. S.: Printed circuit board recycling: Physical processing and copper extraction by selective leaching. *Waste Management.* (2015) <https://doi.org/10.1016/J.WASMAN.2015.08.030>
- [40] Yin, S., Wang, L., Wu, A., Free, M. L., & Kabwe, E.: Enhancement of copper recovery by acid leaching of high-mud copper oxides: A case study at Yangla Copper Mine, China. *J. of Clean. Production.* (2018) <https://doi.org/10.1016/J.JCLEPRO.2018.08.122>